

# A computer vision approach for automated analysis and classification of microstructural image data



Brian L. DeCost, Elizabeth A. Holm\*

*Materials Science and Engineering, Carnegie Mellon University, Pittsburgh, PA 15213, USA*

## ARTICLE INFO

### Article history:

Received 5 May 2015

Received in revised form 5 August 2015

Accepted 6 August 2015

Available online 28 August 2015

### Keywords:

Microstructure

Computer vision

Machine learning

Image data

Feature extraction

## ABSTRACT

The ‘bag of visual features’ image representation was applied to create generic microstructural signatures that can be used to automatically find relationships in large and diverse microstructural image data sets. Using this representation, a support vector machine (SVM) was trained to classify microstructures into one of seven groups with greater than 80% accuracy over 5-fold cross validation. In addition, the bag of visual features was implemented as the basis for a visual search engine that determines the best matches for a query image in a database of microstructures. These novel applications demonstrate the potential and the limitations of computer vision concepts in microstructural science.

© 2015 The Authors. Published by Elsevier B.V. This is an open access article under the CC BY-NC-ND license (<http://creativecommons.org/licenses/by-nc-nd/4.0/>).

## 1. Introduction

Over the past century, materials scientists have made great progress in acquiring, analyzing, and comparing microstructural images [1–22]. Much of the effort has been directed toward deep understanding of particular materials systems or classes of microstructures—and rightly so. When the catalog of possible microstructural features is known or easily enumerated, digital image analysis techniques can take advantage of these well-defined features to segment, characterize, and compare microstructures with high precision. The current paradigm in microstructure analytics is a focus on extracting structure–properties relationships through image descriptors that explicitly describe the shape and appearance of the pertinent microstructural features. A classic example is the characterization of phase volume fraction in two-phase systems. Recent progress has focused on quantifying the phase morphology of fully segmented two-phase systems using higher order point statistics [2]; moment invariant shape descriptors [23,24]; and, more recently, sets of shape descriptors and shape correlation functions that are tailored to particular microstructure systems through a machine learning approach [22].

However, when the feature set or particular features of interest are not known *a priori* or when microstructures differ in significant

or unknown ways, these methods become intractable, inaccurate, or fail completely. For example, image segmentation is the process of assigning each pixel a label designating the microstructural feature to which it belongs (e.g. grain or phase membership). When the catalog of features is not known, the segmentation scheme may not be able to differentiate between a void, a precipitate, and a polishing scratch, for example. Because of this, the choice of an optimal segmentation scheme is highly contingent upon prior knowledge of the material system being analyzed, and for many materials systems no adequate segmentation scheme is known. This limits general applicability of microstructure analysis techniques that operate on segmented images. Likewise, although n-point correlation functions are theoretically able to exactly represent a microstructure, in practice the computational cost increases exponentially with each additional pixel state; performing even 2-point correlation analysis on images with 256 grayscale values is prohibitive. Therefore, these methods are typically applied only to a pre-selected set of micrographs, chosen by a human expert [2,3,6,25,26,22].

In contrast, our goal is to develop a new general method to find useful characteristics and relationships within and between micrographs without any assumptions about what features may be present. Research in the field of computer vision, particularly in image texture recognition applications, has laid the groundwork for this approach. Image texture recognition refers to the task of quantifying the spatial distribution of image intensity in order to identify distinct regions [27]. Some applications include automatic segmentation of satellite imagery [28], automatic differentiation

\* Corresponding author.

E-mail addresses: [bdecost@andrew.cmu.edu](mailto:bdecost@andrew.cmu.edu) (B.L. DeCost), [eaholm@andrew.cmu.edu](mailto:eaholm@andrew.cmu.edu) (E.A. Holm).

between macroscopic surfaces of various materials (such as wood, sandpaper, and cotton) [29], and diagnostic analysis in medical imaging [30]. Commonly used image texture features include Gabor filter banks [31], wavelet transforms [32], characteristic image patches [33], and local image descriptors [34]. An approach based on these well-established computer vision methods can capitalize on the explosion in digital microstructure data over the past two decades to survey the breadth of available microstructures efficiently and without significant human intervention [35–40].

This model of aggregating and systematizing large, diverse data sets is the basis for data science efforts in a variety of fields [41–44]. We are inspired to apply these concepts to microstructural image data by the Never Ending Image Learner (NEIL), which is a computer program that has been analyzing images and text on the web in an attempt to learn visual concepts and common sense relationships between them in a semi-unsupervised manner [45]. Examples of such relationships include “Sparrow is a kind of/looks similar to Bird” or “Horse can be found in Pasture”. The creators of NEIL describe their approach as a form of ‘macro-vision’: extracting statistical patterns and relationships from large collections of images. This is in contrast to ‘micro-vision’, the more traditional computer vision task of extracting information from images on an individual basis. We envision a similar set of tools to enable general studies of the concept of microstructure, within and across materials systems, in contrast to the traditional materials science sense of studying the microstructural features of particular materials systems.

Our primary contribution in this work is to apply established computer vision methods to a diverse collection of microstructure data to develop quantitative microstructure descriptors and methods for defining objective classes of microstructures. The resulting microstructure descriptors can be computed in real-time, and can capture the meaningful details and defining characteristics of microstructural images without explicit fine-tuning from human experts. This constitutes a novel paradigm for microstructure analytics, which complements the current research emphasis on quantitative characterization and design of particular microstructural systems. We hypothesize that this approach to microstructure data will be flexible enough to span a diverse set of materials systems and quantitatively robust enough to enable automatic search and accurate classification of large collections of microstructural image data.

## 2. Microstructure representation

In this exploratory study, we apply the bag of visual features image representation commonly used in the object and scene recognition literature [34,46,47]. This approach is inspired by the bag of words representation for document classification, which models a class of documents as a probability distribution of word occurrences over the set of words in a vocabulary (the English language, for example) [48,49]. Likewise, the bag of visual features representation models a class of images as a probability distribution over a set of visually distinctive features, or ‘visual words’. This image representation can be quickly computed for arbitrary and unsegmented images, yielding a quantitative microstructure representation that requires no *a priori* knowledge of which microstructural features are the most relevant for characterization. The resulting general microstructural representation is well suited for use with a variety of machine learning approaches.

The typical bag of visual features pipeline is split into stages: detection and characterization of local image features [50–52], extraction of a visual dictionary (typically through cluster analysis on a subset of detected features), and construction of the bag of visual features representations [46,47], which can be further ana-

lyzed using a variety of machine learning approaches. The fast-moving field of computer vision offers a wide array of techniques for accomplishing each step in this pipeline, and in practice the performance of any given technique may depend heavily on the application domain. At this early stage of our inquiry, we have chosen a set of techniques with a proven track record of good performance in a variety of applications, keeping in mind that good general microstructure descriptors should be robust against affine image transformations such as changes in scale and orientation. Due to space constraints, we do not attempt to give a comprehensive treatment of the specific computer vision and machine learning techniques that we make use of, which are extensively detailed in the literature.<sup>1</sup>

### 2.1. Detect keypoint features

To localize distinctive microstructural features that will be useful for characterization, we employ the commonly used Harris-Laplace and Difference of Gaussian (DoG) interest point (or keypoint) operators. Both of these interest point operators detect a sparse set of image regions that contain complex image gradient structure. We used VLFeat, a popular open source computer vision library, to compute these interest point operators [54]. The DoG operator localizes blob-like interest points by approximating the image Laplacian at multiple scales using the difference between two Gaussian-smoothed versions of the same image; the scale is set by the variance of the two Gaussians [51]. The Harris-Laplace operator uses the Harris cornerness metric (a combination of determinant and trace of the image intensity Hessian matrix) to detect corner-like interest points, and determines their characteristic scale using the extrema of the multiscale image Laplacian [50]. The resulting set of interest regions that exhibit large image intensity changes in multiple directions, with a characteristic scale that approximately matches the scale of the local image structure [55]. These two interest point operators detect complementary sets of image features [55]. Fig. 1 illustrates the types of keypoints that are localized by these detectors in a pearlitic cast iron microstructure (micrograph 354 from [56]). The size of each circle is corresponds to the characteristic scale of the keypoint feature it represents. Here, the keypoints include large black graphite nodules, the edges of the nodules, pearlitic patches, and so on. These correspond well to the features a materials scientist would likely identify as characteristic of this structure. However, note that keypoint selection is performed on a strictly visual basis, and no physical meaning is construed from them.

### 2.2. Characterize local image features

Many computer vision approaches represent the visual structure of keypoint features through a pattern or distribution of local image gradient values. In this work we use the Scale-Invariant Feature Transform (SIFT) [51,52] as implemented by VLFeat [54]. SIFT is a commonly used keypoint descriptor that offers rotational invariance by using a reference frame that is normalized with respect to the characteristic scale of each individual keypoint feature. Note that the characteristic scale of each keypoint feature is computed during the keypoint detection step. The SIFT descriptor models local visual structure as a histogram of oriented image intensity gradient values in a  $4 \times 4$  grid of spatial bins, each with 8 bins for the image gradient orientation, as shown in Fig. 2. This collection of image gradient histograms is compactly represented

<sup>1</sup> For the interested reader, the introductory text *Computer Vision: Algorithms and Applications* by Richard Szeliski is an excellent primer [53].

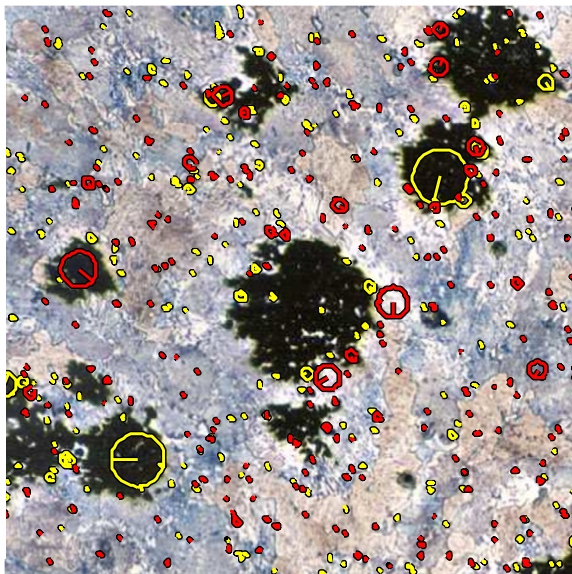


**Fig. 1.** Micrograph of pearlitic cast iron [56] showing keypoints (circles) randomly selected from the 4754 keypoints identified by the Harris-Laplace detector (yellow) and the 8510 keypoints identified by the Difference of Gaussians detector (red). The size of the circle corresponds to the keypoint scale, and the orientation is given by the compass mark. (For interpretation of the references to color in this figure legend, the reader is referred to the web version of this article.)

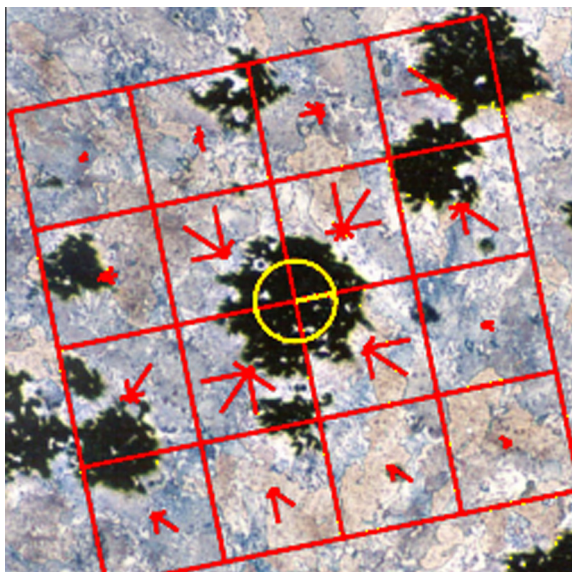


**Fig. 2.** Graphical depiction of the SIFT descriptor corresponding to the central black nodule (circle). Average intensity gradients (arrows) are calculated for each box in a  $4 \times 4$  grid of bins surrounding the feature. Each bin contains 8 sub-bins for the gradient orientation.

by a 128-dimensional vector, which can conveniently serve as input to a variety of machine learning algorithms.

### 2.3. Extract a visual dictionary

The bag of visual features approach treats an image as a collection of local image gradient patterns, each of which is represented by a high-dimensional vector that characterizes the local visual appearance of a keypoint feature. This high-dimensional feature space is quantized into a visual vocabulary to allow for fast matching and application of information retrieval techniques. A visual

vocabulary is obtained by performing cluster analysis on a random subset of keypoint descriptors extracted from a representative training set of images. We used  $k$ -means clustering [57,58] with 100 clusters to quantize the SIFT descriptors extracted from the full training set for all of the current experiments. The cluster centers represent the visual words that make up the vocabulary. The optimal choice of  $k$ , the number of clusters, can be highly sensitive to the size and visual content of the image dataset. Although several means of selecting a value for  $k$  exist, there is no consensus over which method is ‘correct’ [59]. In computer vision applications, generally larger codebooks yield higher performance, and the value for this parameter is often simply tuned in an Edisonian fashion by interrogating the cross-validation performance of a classifier system trained with varying values of  $k$ , though care must be taken to avoid overfitting [47]. Because we have a relatively small classification dataset, we make no attempt to optimize  $k$  here, but recognize this as an area for future investigation. The result for our current classification dataset is the visual dictionary of 100 features shown in Fig. 3. It is apparent that this dictionary contains features corresponding to dark circles, textured regions, dark lines, line junctions, and feature edges, as well as other less obvious visual words.

A single visual dictionary is extracted from a set of images containing the full range of microstructural variation pertinent to the task at hand. Thus, for a study of related materials systems (i.e. alloys), examples of each materials system of interest should be included in the training set used to construct the visual dictionary. For a general study of all materials systems (i.e. the archives of a materials science journal), a representative sample of all the microstructural images appearing in the dataset should be used to construct the visual dictionary.

### 2.4. Construct microstructural fingerprints

The bag of visual features representation for an image is a normalized histogram measuring the frequency of each visual word in the image. Each keypoint feature counts as an instance of the visual word corresponding to the closest cluster center in the visual dictionary, as illustrated in Fig. 4. Thus, the image histogram is a ‘fingerprint’ of the microstructure that generated it. We compare image histograms using the  $\chi^2$  distance, which is a metric for quantifying the difference between two histograms that performs well for image texture recognition applications [60]. For two  $m$ -bin histograms  $X = (x_1, \dots, x_m)$  and  $Y = (y_1, \dots, y_m)$  the  $\chi^2$  distance is:

$$D(X, Y) = \frac{1}{2} \sum_{i=1}^m \frac{(x_i - y_i)^2}{x_i + y_i} \quad (1)$$

Just as in fingerprint matching, the smaller the difference between image histograms (therefore the more features in common), the more similar two microstructures are presumed to be. Naturally, below a certain threshold, two similar microstructures could have indistinguishable bag of features histograms. Note that the microstructure representation we use here does not capture spatial correlations between microstructural features in any way.

## 3. Results and discussion

Microstructures vary widely across different materials systems and processing history, and there is currently no easy way to automatically sort and classify them. We have performed a small classification experiment to demonstrate the utility (and evaluate the effectiveness) of the bag of visual features representation as a general microstructure descriptor. We also used the bag of visual features representation to rank the images in a microstructure database on the basis of microstructural similarity. We used separate visual dictionaries for each application: In the classification

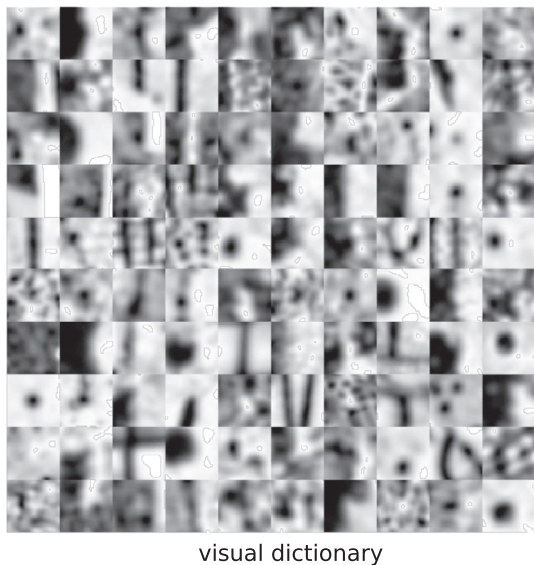


**Fig. 3.** Representative image patches corresponding to the 100-word visual dictionary extracted from our 7-category classification dataset with  $k$ -means clustering.

experiment, the visual dictionary was extracted from the training set of microstructures. In the microstructure similarity experiment, the visual dictionary was extracted using the entire microstructure database as the source of keypoint features.

### 3.1. Microstructure classification

Using an internet search engine, we manually collected and labeled a small dataset consisting of 105 micrographs belonging to the seven distinct classes of microstructure shown in Fig. 5: brass, ductile cast iron, gray cast iron, hypoeutectoid steel, malleable cast iron, superalloy, and annealing twins. We demonstrate the utility of the bag of words microstructure representation by using it to train a support vector machine (SVM) [61,62] classifier using the  $\gamma^2$  kernel [60]. This classifier can automatically discriminate between these seven different microstructure classes.

The SVM is a machine learning classifier that is commonly used in computer vision applications. We used the one-vs-all scheme for multi-class SVM classification [63]: for each image class, one SVM classifier is trained to distinguish that class from all other classes. To predict the class of a previously unseen test image, the class prediction by each classifier is computed given the bag of words representation of the test image, and the test image is assigned according to the prediction with the highest confidence. We used scikit-learn, a popular machine learning library, for SVM classification [64].

We performed our classification experiment using a stratified 5-fold cross-validation scheme, a method for using all available data for training without sacrificing unbiased measurements of accuracy [59]. We partition the complete dataset into five *folds*, each consisting of 21 images (three images per microstructure class). For each of the five folds, we train a classifier system on a training set consisting of the remaining four folds. We measure the performance of this classifier system using a validation set that consists of the fold that was excluded from the current training set. Thus each of the 105 images in the dataset is used for training the classifier four times, and appears in a validation set exactly once. The overall accuracy estimate is the average accuracy out of the five cross-validation folds.

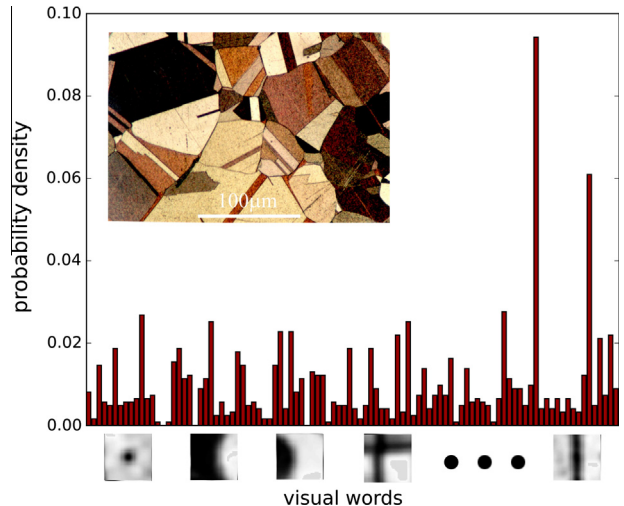


**Fig. 4.** The bag of microstructural words histogram for the highly twinned microstructure (inset, micrograph 430 from [56]). Each bin along the horizontal axis corresponds to a visual word, as schematically indicated. This histogram is the microstructural fingerprint of the image.

Our classifier system achieves a 5-fold cross-validation accuracy of 83% with standard deviation 3%. The confusion matrix in Fig. 6 graphically shows the classification performance with respect to each individual class: The vertical axis corresponds to the true class of each validation image, and the horizontal axis corresponds to the class predicted by the SVM classifier. Thus correct classifications lie along the diagonal of the confusion matrix. For example, three of the micrographs with annealing twins were misclassified as gray cast iron, while two micrographs of superalloy were misclassified as the annealing twin class. The misclassification between annealing twins and gray cast iron is interesting because of the preponderance of straight line features in both classes of microstructure. In contrast, every brass image was correctly classified, and only one micrograph (a gray cast iron) was misclassified as brass.

Due to our limited dataset size, we have made no efforts to tune model hyper-parameters such as the number of visual words or the SVM regularization parameter, which would require an additional cross-validation loop. This is primarily to avoid overfitting to the relatively small dataset, which would result in overestimation of the generalization performance of our classifier system. Nonetheless, these results demonstrate the potential for machine vision approaches to microstructural classification. Even using untuned model parameters and a small training set, the system achieves impressively accurate classification performance without human intervention, compared with a random-guessing accuracy of about 14%. This is somewhat lower than the performance of state of the art texture recognition systems evaluated on commonly used image texture datasets. For many datasets, the state of the art texture recognition performance is in the high 90% range [29]. However, these datasets are larger and carefully collected. We expect that with further optimization of our method, future quantitative microstructure studies can achieve similar performance. Additionally, even our current performance results are sufficient to support data mining on historical archives of microstructural images. In fact, this method is the only current candidate to search and/or classify sets of arbitrary, unsegmented micrographs.

### 3.2. Microstructural similarity ranking

The bag of visual features microstructure representation also unlocks the potential for novel microstructural data mining

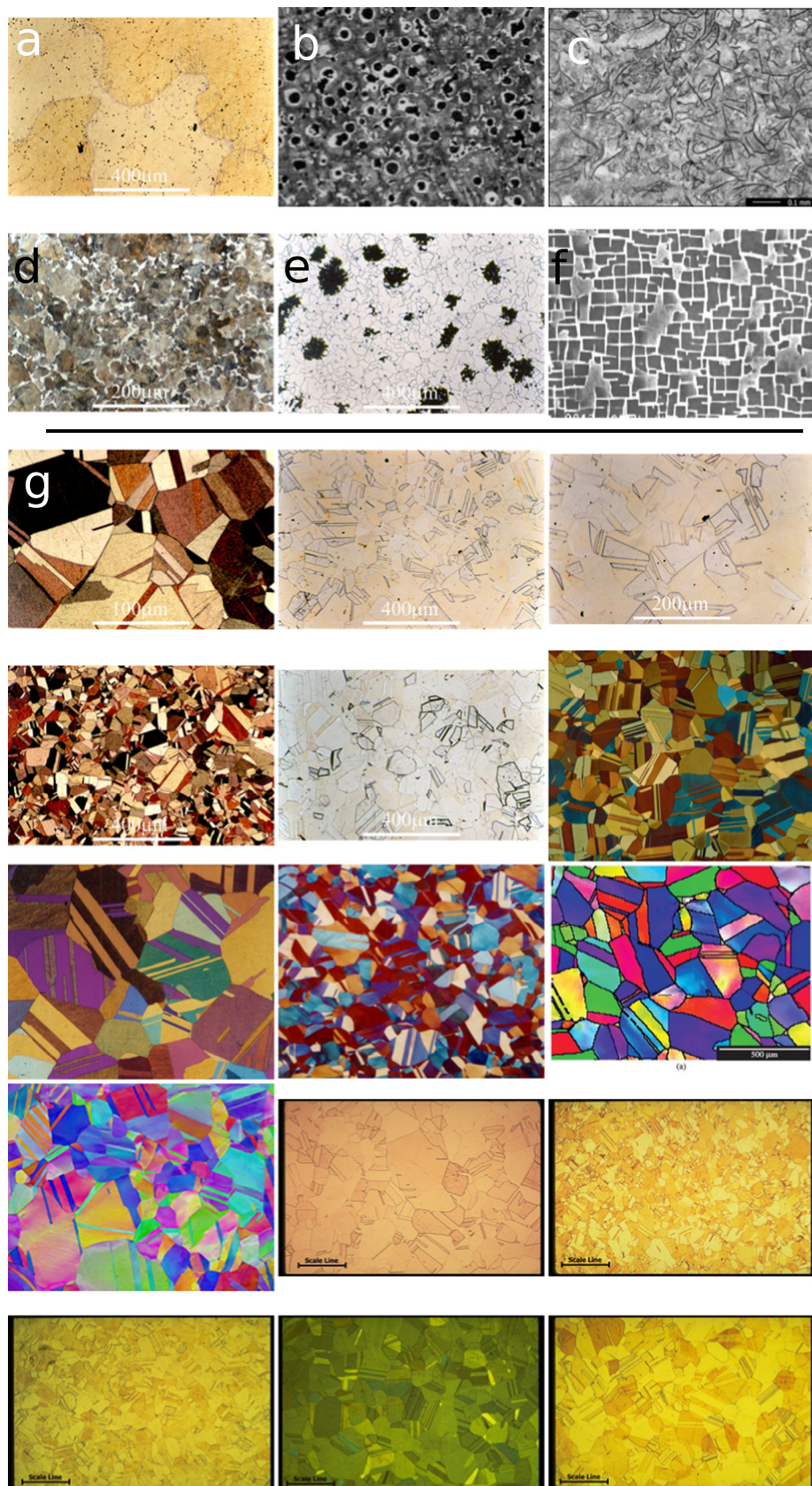


**Fig. 5.** Example microstructures for the seven microstructure classes used in the classification test. (a) Brass/bronze, (b) ductile cast iron, (c) gray cast iron, (d) hypoeutectoid steel, (e) malleable cast iron, (f) superalloy and (g) all 15 annealing twin images.

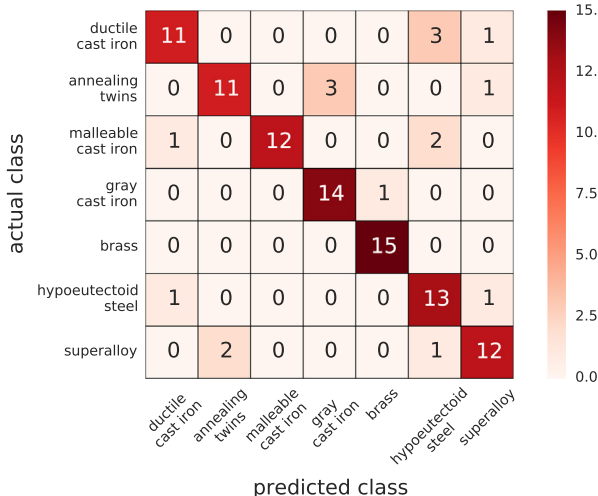


**Fig. 6.** Confusion matrix showing performance of the microstructural classification scheme. For micrographs in a particular actual class, the rows tally the predicted class assignments by the microstructure classifier. The upper-left to lower-right diagonal entries give the number of accurate classifications for each actual class.

approaches. One example is a visual search engine for exploring a microstructure database. We demonstrate this concept by visually indexing 772 microstructure images from the Cambridge DoIT-PoMS micrograph library [56], again using the  $\chi^2$  kernel [60] to compare microstructure signatures. Fig. 7 shows the closest four matches in the database for five example queries. Bear in mind that this database is meant for teaching applications, and is thus relatively sparse: many materials systems are represented by just two or three examples. The first row shows a brass query microstructure which returns four visually similar brass microstructures. The second row shows an alumina-graphite composite microstructure that matches closely with another magnesium oxide-graphite composite, and then two steel microstructures that appear to have similar visual texture, and finally a gun metal bronze—a very different material system that contains some visually similar globular features. The third row shows a dendritic steel microstructure that returns four more steel and cast iron microstructures that share visual features with the query, but the overall scales between the images differ substantially. The fourth row shows a series of ductile iron micrographs with prominent spheroidal graphite inclusions. The fourth-closest match found is a hypoeutectoid steel, which has similar visual texture. The fifth row shows a close view of dendritic cast iron, which returns much broader views of similar dendritic cast irons and TRIP steels. Again, although this system has not yet been optimized, these results are encouraging. Given a query image, the search engine returns microstructures that are objectively related to it, and often the relationship is subjectively obvious as well.

### 3.3. Applications

The bag of visual features representation is a general microstructure descriptor that presumes nothing about the material system or microstructural features of interest. Instead, the computer system learns a set of discriminative microstructural features from the data itself. The underlying feature descriptors are robust to changes in scale, orientation, and overall illumination or imaging conditions. These qualities are critical for automatically comparing images of disparate microstructural classes at a variety of magnifications or physical scales, in an arbitrary body of microstructural data. Once a visual dictionary has been learned from a training set of microstructural images, the bag of visual fea-

tures representations can be quickly computed; SIFT and related computer vision techniques are computationally efficient enough for real-time video analysis applications [65–67].

Applying the bag of visual features representation to microstructure images enables a variety of outcomes based on machine learning, which could provide new ways for materials scientists to study relationships between broad classes of microstructures and materials. Indeed, a general quantitative microstructure representation could allow materials scientists to define objective classes of microstructure. Microstructural classification and search methods could be used to organize, search, and mine microstructural databases in order to unlock the wealth of information stored in academic, industrial, and journal archives [39]. Furthermore, the bag of visual words representation could extend quantitative microstructure–properties investigations to microstructural systems which are not readily segmented. If microstructural images are linked to metadata such as processing conditions and material properties, machine learning methods could be used to extract microstructure–processing–properties relationships, a key element of creating materials by design [68,69]. Finally, quickly computed quantitative microstructure representations combined with automated metallography could enable online microstructure monitoring for applications in industrial process control systems. In each case, the key element is automated and quantitative characterization of microstructural images, efficiently and without human intervention.

### 3.4. Limitations

Though the bag of visual features microstructure representation is an efficiently computed quantitative microstructure descriptor, it is ultimately an approximate measure of the visual structure of a micrograph rather than an objective measure of the physical structure of the analyte material. Thus any microstructure relationships extracted using this approach are likely to be empirical in nature, and correlative rather than causative. Furthermore, our current approach is strongly rooted in representing microstructural images as visual textures or scenes. This model is not appropriate for understanding micrographs that are not representative of their class, particularly closeups of individual features or high resolution transmission electron micrographs. These kinds of micrographs are problematic in general for all statistical characterization methods, because they contain a scan area that is smaller than the representative volume element (RVE) at the pertinent length scale. However, the bag of visual features histogram could be used as a convergence metric to help determine the RVE size for future microstructure studies.

Microstructural images may contain considerable data that are not included in the bag of visual words representation. For example, while color is often used to indicate crystallography, composition, phase, etc., the feature descriptors utilized here operate on intensity gradients only and ignore absolute color. Likewise, although the scale-invariant nature of the bag of visual features makes it robust with respect to analyzing images at different physical scales or magnification (and even to evaluating microstructures where no scale information is available), the physical scale of microstructural features may be important both for comparing microstructures and for correlating with physical properties. Finally, the bag of visual features representation makes no attempt to assess spatial relationships between microstructural features, such as proximity, directionality, or clustering. Clearly, incorporating these important and influential microstructural aspects into the image representation is an opportunity for future work.

On a broader scale, many computer vision systems are most effective when applied to web-scale data: for example, the NEIL project has analyzed more than two million images gathered from

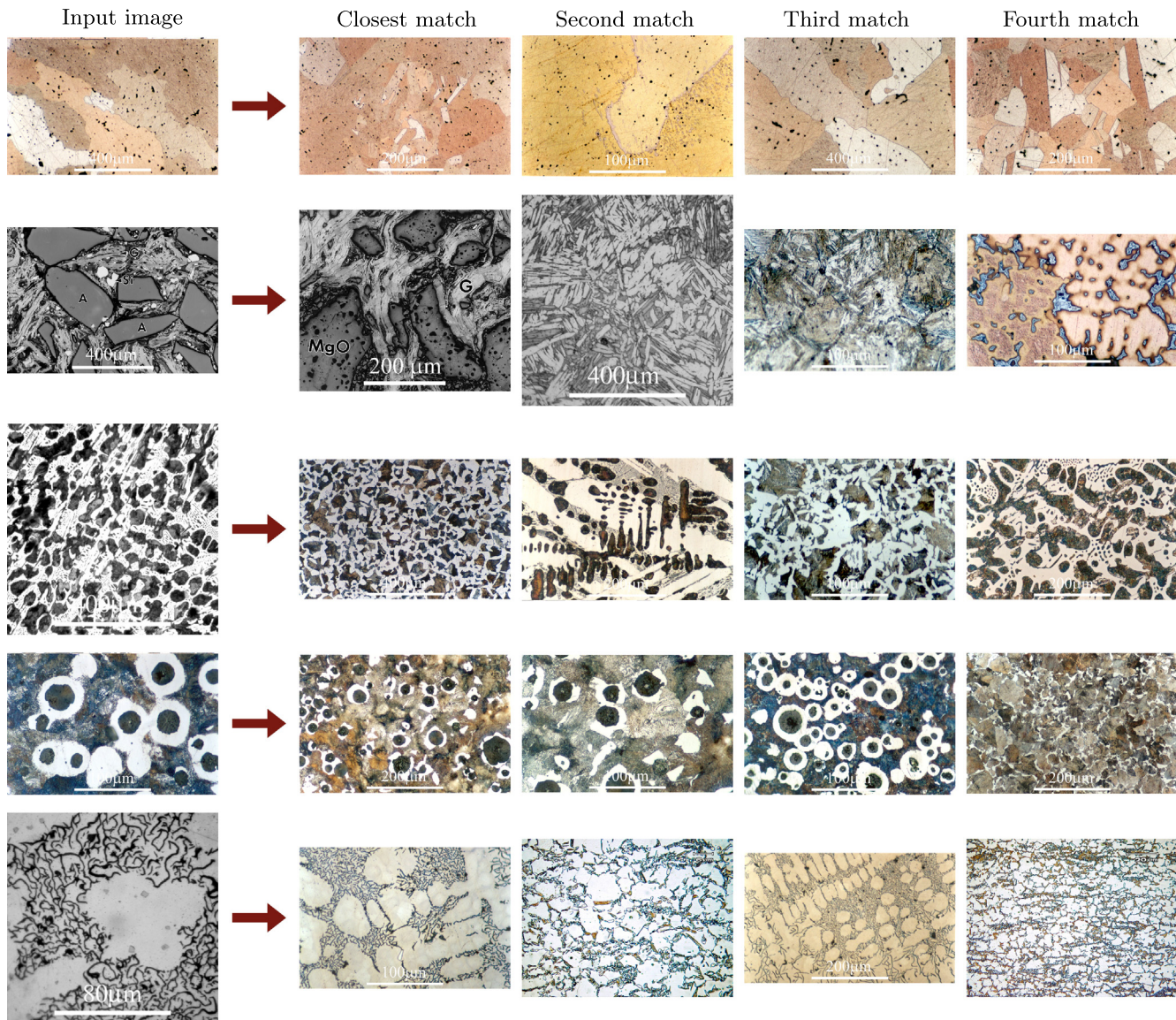


**Fig. 7.** Results of the visual microstructure search of the DoITPoMS micrograph library [56] for five query images (left column). The right four columns show the top four matches for each query image.

the internet [45]. A large dataset both improves fidelity and enables additional analyses, such as multi-label classification (i.e. a dendritic structure may also be a metal alloy). Though materials scientists and metallurgists have been collecting micrographs for over 100 years, compared to web-scale image data the full set of microstructure data is quite small. While much of this data set exists in digital form, it is fragmented across various academic and industrial archives. Open microstructure databases are a critical need for the advancement of microstructural data mining, both to provide a large enough dataset for meaningful algorithmic development and validation, and to foster a healthy microstructure informatics community.

#### 4. Conclusions

The problem of structuring and managing large microstructural databases in a way that enables the synthesis of microstructural knowledge is very much an open one [35–40]. We show that the bag of visual features image representation can be used to compute microstructural fingerprints that capture the defining features of

individual microstructures. By comparing the histograms of visual features, a support vector machine (SVM) can classify microstructures into groups automatically and with high accuracy, even using relatively small training data sets. In addition, the feature histogram can provide the basis for a visual search engine that finds the best matches for a query image in a database of microstructures. Ultimately, this automatic and objective computer vision system offers a new approach to archiving, analyzing, and utilizing microstructural data.

#### Acknowledgments

This work was supported in part by the National Science Foundation under grant DMR-1307138. B.L.D. would also like to acknowledge the support of the John and Claire Bertucci Graduate Fellowship Foundation. We would also like to thank Professor Abhinav Gupta and Xinlei Chen of the Carnegie Mellon University School of Computer Science for stimulating conversation, advice, and inspiration through their work on the NEIL project.

## References

- [1] David W. Rosen, Namin Jeong, Yan Wang, *Comput.-Aided Des.* 45 (7) (2013) 1068–1078.
- [2] S.R. Kalidindi, D.T. Fullwood, *JOM* 59 (9) (2007) 26–31.
- [3] Surya R. Kalidindi, Stephen R. Niezgoda, Ayman A. Salem, *JOM* 63 (4) (2011) 34–41.
- [4] S.R. Niezgoda, D.T. Fullwood, S.R. Kalidindi, *Acta Mater.* 56 (18) (2008) 5285–5292.
- [5] G. Saheli, H. Garmestani, B.L. Adams, *J. Comput.-Aided Mater. Des.* 11 (2–3) (2004) 103–115.
- [6] Stephen R. Niezgoda, Anand K. Kanjrala, Surya R. Kalidindi, *Integrating Mater. Manuf. Innovat.* 2 (1) (2013) 1–27.
- [7] Ossama B. Abouelatta, *J. Am. Sci.* 9 (6) (2013).
- [8] D.T. Fullwood, S.R. Kalidindi, S.R. Niezgoda, A. Fast, N. Hampson, *Mater. Sci. Eng.: A* 494 (1) (2008) 68–72.
- [9] Thiago M. Nunes, Victor Hugo C. De Albuquerque, Joao P. Papa, Cleiton C. Silva, Paulo G. Normando, Elineudo P. Moura, Joao Manuel R.S. Tavares, *Expert Syst. Appl.* 40 (8) (2013) 3096–3105.
- [10] Cyril Stanley Smith, *A History of Metallography—the Development of Ideas on the Structure of Metals before 1890*, The University of Chicago Press, 1960.
- [11] Umesh Adiga, Murali Gorantla, James Scott, Daniel Banks, Yoon-Suk Choi, Building 3d microstructure database using an advanced metallographic serial sectioning technique and robust 3d segmentation tools, in: *Proceedings of the 2nd World Congress on Integrated Computational Materials Engineering (ICME)*, John Wiley & Sons, 2013, p. 243.
- [12] Mary Comer, Charles A. Bouman, Marc De Graef, Jeff P Simmons, *JOM J. Miner. Met. Mater. Soc.* 63 (7) (2011) 55–57.
- [13] E. Gulsoy, M. Degraef, *Microscopy Microanal.* 15 (S2) (2009) 606–607.
- [14] W.B. Lievers, A.K. Pilkey, *Mater. Sci. Eng.: A* 381 (1) (2004) 134–142.
- [15] Aleks Y.M. Ontman, Gary J. Shiflet, *Metall. Mater. Trans. A* 41 (9) (2010) 2236–2247.
- [16] Pattan Prakash, V.D. Mytri, P.S. Hiremath, *Microscopy Microanal.* 17 (06) (2011) 896–902.
- [17] Veeraghavan Sundaraghavan, Nicholas Zabaras, *Computat. Mater. Sci.* 32 (2) (2005) 223–239.
- [18] George F. Vander Voort, *Metallography – Past, Present, and Future: 75th Anniversary Volume*, vol. 11, Astm International, 1993.
- [19] Jarrell Waggoner, Youjie Zhou, Jeff Simmons, Marc De Graef, Song Wang, *IEEE Trans. Image Process.* 22 (12) (2013) 5282–5293.
- [20] Cyril Stanley Smith, *Trans. Metall. Soc. AIME* 175 (1948) 15–51.
- [21] J. Warren, L. Freidersdorf, in: *Materials Science and Technology: MS&T'14*, TMS, October 2014.
- [22] Hongyi Xu, Ruochuan Liu, Alok Choudhary, Wei Chen, *J. Mech. Des.* 137 (5) (2015), 051403-1–051403-10.
- [23] J.P. MacSleynne, J.P. Simmons, M. De Graef, *Acta Mater.* 56 (3) (2008) 427–437.
- [24] J.P. MacSleynne, J.P. Simmons, M. De Graef, *Modell. Simul. Mater. Sci. Eng.* 16 (4) (2008) 045008.
- [25] Stephen R. Niezgoda, Surya R. Kalidindi, Xiaohua Hu, Gordana A. Cingara, David S. Wilkinson, Mukesh Jain, Peidong Wu, Raja K. Mishra, M. Arifin, J. Szpunar, *Mater. Continua* 14 (2) (2010) 79–98.
- [26] M.A. Tschopp, M.A. Groeber, R. Fahringer, J.P. Simmons, A.H. Rosenberger, C. Woodward, *Modell. Simul. Mater. Sci. Eng.* 18 (2) (2010) 025014.
- [27] Robert M. Haralick, Karthikeyan Shanmugam, Its' Hak Dinstein, *IEEE Trans. Syst., Man Cybernet. SMC-3* (6) (1973) 610–621.
- [28] A.P. Carleer, Olivier Debeir, Eléonore Wolff, *Photogramm. Eng. Remote Sens.* 71 (11) (2005) 1285–1294.
- [29] Barbara Caputo, Eric Hayman, Mario Fritz, Jan-Olof Eklundh, *Image Vision Comput.* 28 (1) (2010) 150–163.
- [30] Tim F. Cootes, Christopher J. Taylor, in: *Medical Imaging 2001*, International Society for Optics and Photonics, 2001, pp. 236–248.
- [31] S. Livens, P. Scheunders, G. Van de Wouwer, D. Van Dyck, *Sixth International Conference on Image Processing and Its Applications*, vol. 2, IET, 1997, pp. 581–585.
- [32] Michael Unser, *IEEE Trans. Image Process.* 4 (11) (1995) 1549–1560.
- [33] Manik Varma, Andrew Zisserman, *IEEE Trans. Pattern Anal. Mach. Intell.* 31 (11) (2009) 2032–2047.
- [34] Svetlana Lazebnik, Cordelia Schmid, Jean Ponce, *IEEE Trans. Pattern Anal. Mach. Intell.* 27 (8) (2005) 1265–1278.
- [35] National Research Council, *Big Data in Materials Research and Development: Summary of a Workshop*, The National Academies Press, Washington, DC, 2014.
- [36] J. Warren, R.F. Boisvert, *Workshop Report: Building the Materials Innovation Infrastructure: Data and Standards*, Technical Report NISTIR 7898, National Institute of Standards and Technology, November 2012.
- [37] Ad-hoc Interagency Group on Advanced Materials, *Materials Genome Initiative for Global Competitiveness*, National Science and Technology Council OSTP, July 2011, pp. 1–18.
- [38] National Research Council Committee on Integrated Computational Materials Engineering, *Integrated Computational Materials Engineering: A Transformational Discipline for Improved Competitiveness and National Security*, The National Academies Press, Washington, DC, 2008.
- [39] Subcommittee on the Materials Genome Initiative, *Materials Genome Initiative Strategic Plan*, Technical Report NISTIR 7898, National Institute of Standards and Technology, Washington, DC, USA, December 2014.
- [40] P. Bajcsy, Y. Khalidi, H. Peng, K.D. Borne, in: *Big Data Science: BigData'14*, TMS, October 2014.
- [41] Doug Howe, Maria Costanzo, Petra Fey, Takashi Gojobori, Linda Hannick, Winston Hide, David P. Hill, Renate Kania, Mary Schaeffer, Susan St. Pierre, *Nature* 455 (7209) (2008) 47–50.
- [42] Kieran Jay Edwards, Mohamed Medhat Gaber, *Astronomy and Big Data*, vol. 6, Springer, New York, 2014.
- [43] Geoff Brumfiel, *Nature* 469 (20) (2011) 282–283.
- [44] A. Kassner, R.E. Thornhill, *Am. J. Neuroradiol.* 31 (5) (2010) 809–816.
- [45] Xinlei Chen, Abhinav Shrivastava, Abhinav Gupta, Neil: extracting visual knowledge from web data, in: *2013 IEEE International Conference on Computer Vision (ICCV)*, IEEE, 2013, pp. 1409–1416.
- [46] Gabriella Csurka, Christopher Dance, Lixin Fan, Jutta Willamowski, Cédric Bray, *Workshop on Statistical Learning in Computer Vision*, vol. 1, ECCV, 2004, pp. 1–2.
- [47] Eric Nowak, Frédéric Jurie, Bill Triggs, in: *Computer Vision – ECCV 2006*, Springer, 2006, pp. 490–503.
- [48] Hans Peter Luhn, *IBM J. Res. Dev.* 2 (2) (1958) 159–165.
- [49] Gerard Salton, Michael J. McGill, *Introduction to Modern Information Retrieval*, McGraw-Hill, Inc., 1986.
- [50] Krystian Mikolajczyk, Cordelia Schmid, *Proceedings. Eighth IEEE International Conference on Computer Vision, 2001. ICCV 2001*, vol. 1, IEEE, 2001, pp. 525–531.
- [51] David G. Lowe, *The Proceedings of the Seventh IEEE International Conference on Computer Vision*, vol. 2, IEEE, 1999, pp. 1150–1157.
- [52] David G. Lowe, *Int. J. Comput. Vision* 60 (2) (2004) 91–110.
- [53] Richard Szeliski, *Computer Vision: Algorithms and Applications*, Springer, 2010.
- [54] Andrea Vedaldi, Brian Fulkerson, in: *Proceedings of the International Conference on Multimedia*, ACM, 2010, pp. 1469–1472.
- [55] Krystian Mikolajczyk, Cordelia Schmid, *Int. J. Comput. Vision* 60 (1) (2004) 63–86.
- [56] Z.H. Barber, J.A. Leake, T.W. Clyne, *J. Mater. Educ.* 29 (1/2) (2007) 7.
- [57] Stuart Lloyd, *IEEE Trans. Inform. Theory* 28 (2) (1982) 129–137.
- [58] David Arthur, Sergei Vassilvitskii, in: *Proceedings of the Eighteenth Annual ACM-SIAM Symposium on Discrete Algorithms*, Society for Industrial and Applied Mathematics, 2007, pp. 1027–1035.
- [59] Trevor Hastie, Robert Tibshirani, Jerome Friedman, T. Hastie, J. Friedman, R. Tibshirani, *The Elements of Statistical Learning*, vol. 2, Springer, 2009.
- [60] Jianguo Zhang, Marcin Marszałek, Svetlana Lazebnik, Cordelia Schmid, *Int. J. Comput. Vision* 73 (2) (2007) 213–238.
- [61] Corinna Cortes, Vladimir Vapnik, *Mach. Learn.* 20 (3) (1995) 273–297.
- [62] Bernhard Schölkopf, Alexander J. Smola, *Learning with Kernels: Support Vector Machines, Regularization, Optimization, and Beyond*, MIT Press, 2002.
- [63] Chih-Wei Hsu, Chih-Jen Lin, *IEEE Trans. Neural Networks* 13 (2) (2002) 415–425.
- [64] Fabian Pedregosa, Gaël Varoquaux, Alexandre Gramfort, Vincent Michel, Bertrand Thirion, Olivier Grisel, Mathieu Blondel, Peter Prettenhofer, Ron Weiss, Vincent Dubourg, *J. Mach. Learn. Res.* 12 (2011) 2825–2830.
- [65] Herbert Bay, Andreas Ess, Tinne Tuytelaars, Luc Van Gool, *Comput. Vision Image Underst.* 110 (3) (2008) 346–359.
- [66] Sudipta N. Sinha, Jan-Michael Frahm, Marc Pollefeys, Yakup Genc, in: *EDGE, Workshop on Edge Computing Using New Commodity Architectures*, vol. 278, 2006, p. 4321.
- [67] Kristen Grauman, Trevor Darrell, *The pyramid match kernel: discriminative classification with sets of image features*, *Tenth IEEE International Conference on Computer Vision*, 2005. ICCV 2005, vol. 2, IEEE, 2005, pp. 1458–1465.
- [68] Gregory B. Olson, *Science* 277 (5330) (1997) 1237–1242.
- [69] Gregory B. Olson, *Science* 288 (5468) (2000) 993–998.